Characterisation of Mechanical Properties Using Ball Indentation, Small Punch Creep and Impression Creep Methods

M.D. Mathew

Abstract Tensile and creep properties of materials are usually evaluated using standard test methods. These methods are material intensive. Small specimen testing methods such as, Impression Creep, Small Punch Creep and Ball Indentation allows us to determine the mechanical properties of materials. Creep deformation behavior can be studied using Impression Creep. Small Punch Creep test method is used to evaluate creep deformation and fracture properties of materials. Tensile properties and fracture toughness can be evaluated using Ball Indentation method. Compared to the standard test methods, these methods have several advantages in materials development, structural integrity assessment and characterization of mechanical properties of different but narrow microstructural zones in weld joints. This paper presents a review of the recent advances in these three small specimen testing methods and discusses their relative advantages and limitations using ferrous and non-ferrous alloys.

Keywords Impression creep · Small punch creep · Ball indentation · Creep · Nitrogen

Introduction

Evaluation of tensile, creep and impact properties of materials is carried out by destructive mechanical tests using bulk samples. The sample size and testing procedures are given in the international testing standards. Several innovative small specimen testing techniques are also under development for evaluation of mechanical properties of materials such as Impression Creep (IC), Small Punch Creep (SPC) and Ball Indentation (BI) methods. When compared with standard

M.D. Mathew (✉)
Saintgits College of Engineering, Kottayam, India
e-mail: mdmathew@gmail.com

M.D. Mathew
Indira Gandhi Center for Atomic Research, Kalpakkam, India

mechanical tests, these test techniques have many advantages and unique appli-cations: (a) These methods require only a small amount of material for the tests. Hence these are attractive for remnant life assessment studies where removing large amount of material from an operating component will impair its integrity; (b) rapid screening of mechanical properties can be done by using small laboratory heats for optimising the chemical composition in material development programme; (c) be-ing a localized testing technique, characterization of mechanical properties of narrow microstructural regions that exist in the heat affected zones in weld joints can be carried out; and (d) large amount of data can be collected from one small sample which not only reduces the time and cost of sample preparation, but also reduces the sample to sample variation in properties. Nevertheless, these test techniques have limitations too. (a) Nature of loading is compressive or bending unlike in conventional mechanical tests in which the loading mode is tensile; (b) the test time is generally short, and so is not sensitive to long term microstructural changes in alloys which occur at high temperatures; and (c) interpretation of the results is difficult on account of the complex localization and multi-axial nature of the stresses developed. This paper summarizes some of the research work carried out by the author using Impression Creep, Small Punch Creep and Ball Indentation test methods.

Impression Creep

Impression creep tests are carried out to evaluate the creep deformation behavior of materials. The technique was pioneered by JCM Li and co-workers [1–3]. In an Impression Creep test, a cylindrical punch typically of 1 mm diameter with a flat end, made of tungsten carbide, is forced into the flat surface of a sample of about $10 \times 10 \times 10$ mm by the application of a constant load and at high temperature. During the test, the penetration of the cylindrical punch is continuously monitored as a function of time till a steady state is reached.

When a constant load L is applied to the specimen through a cylindrical punch of diameter d, the mean pressure under the punch is given by,

$$\sigma_{imp} = \frac{4L}{\pi d^2}.$$

(1)

Under the stress σ_{imp}, the cylindrical punch penetrates into the surface of the specimen to a depth h in time t. The rate at which the cylindrical punch penetrates the specimen surface is referred to as impression velocity. It is given by,

$$v_{imp} = \frac{dh}{dt}.$$

(2)

Empirical correlations have been developed for σ_{imp} and $\frac{v_{imp}}{d}$ (normalised impression velocity) in impression creep and uniaxial stress σ_{uni} and creep rate $\dot{\varepsilon}_{uni}$ in conventional uniaxial creep respectively [4]. The general forms of these correlations are [5],

$$\sigma_{uni} = \alpha\sigma_{imp} \tag{3}$$

$$\dot{\varepsilon}_{uni} = \frac{v_{imp}}{\beta d} \tag{4}$$

where, α and β are the correlation factors. α has a value of about 0.3 for most materials and the value of $\beta = 1$.

A typical impression creep testing system is shown in Fig. 1a. It consists of a specimen cage with two frames, one fixed to the bottom plate of the specimen cage and the other connected to the pull rod which is free to move. The former has an indenter holder to which the indenter is fixed and the latter has a sample holder over which test specimen is placed below the indenter. The pull rod is connected to the lever arm which has a 1:10 lever ratio. The vertical movement of the pull rod and hence the impression depth is sensed through a Linear Variable Differential Transducer. A load cell is attached to the load train in order to measure the applied load accurately. The temperature control system ensures constant temperature. The furnace is surrounded by a vacuum chamber which can produce a vacuum level up to 10^{-6} mbar and is used to avoid oxidation of the specimen at higher test temperatures. Impression creep data is recorded using a PC-based online data acquisition system. Typical indentations from IC tests are shown in Fig. 1b.

Alloy Development Studies Using Impression Creep

One of the potential applications of impression creep technique is to rapidly evaluate the creep properties of a large number of laboratory heats while optimizing the chemical composition for developing a new alloy. Impression creep technique was used to optimize the nitrogen content in 316LN SS for enhanced creep properties [6]. Figure 2 shows the variation of steady state impression velocity with nitrogen content at different load levels at a temperature of 923 K. The steady state impression velocity decreased with increasing nitrogen content. This trend was in good agreement with the results obtained from conventional uniaxial creep tests which showed a decrease in steady state creep rate with increase in nitrogen content [7]. Nitrogen is an interstitial solid solution strengthener and it is known to improve tensile, creep and fatigue strength of austenitic stainless steels [8].

Fig. 1 a Impression creep testing system. **b** Typical impressions from IC tests carried out at 923 K on 316LN SS
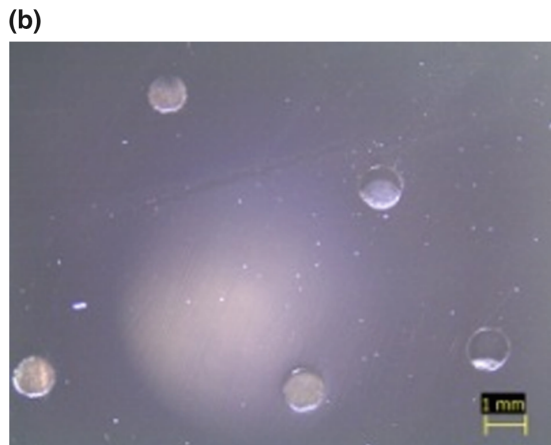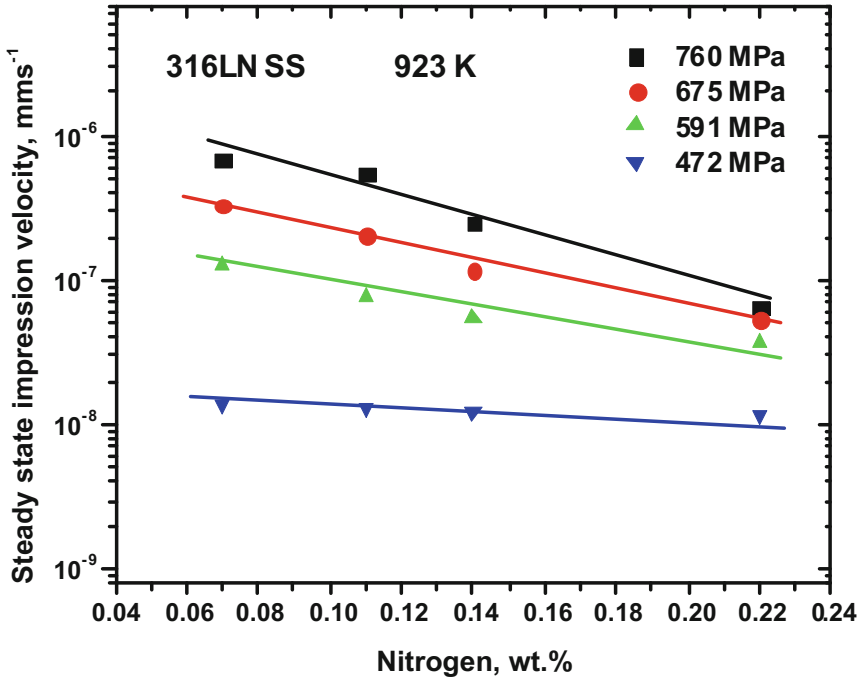
Fig. 2 Decrease in steady state impression velocity by increasing nitrogen content in 316LN SS at various stress levels tested at 923 K

Characterization of Creep Properties of Weld Joints

Impression creep technique is especially useful to study the creep properties of narrow and different microstructural regions in a weld joint which cannot be determined from conventional creep tests. Several researchers have successfully employed the impression creep technique to characterize creep properties of different microstructural zones of weld joints [9]. Impression creep tests were carried out at 923 K on the weld metal, the heat affected zone and the base metal of a single block of 316LN SS weld joint [10]. The microstructure of the base metal was characterized by equiaxed grains while the heat-affected zone had coarse grains. Microstructure of the weld metal consisted of austenite and δ-ferrite. Figure 3a shows the impression creep curves for the three different regions. The variation of impression velocity with time for the weld metal, the base metal and the heat-affected zone (HAZ) regions at 923 K under a punching stress level of 760 MPa is shown in Fig. 3b. Impression velocity was found to initially decrease with time and then attain a constant value indicating a steady state creep stage. Weld metal region showed a higher steady state impression velocity than the base metal.
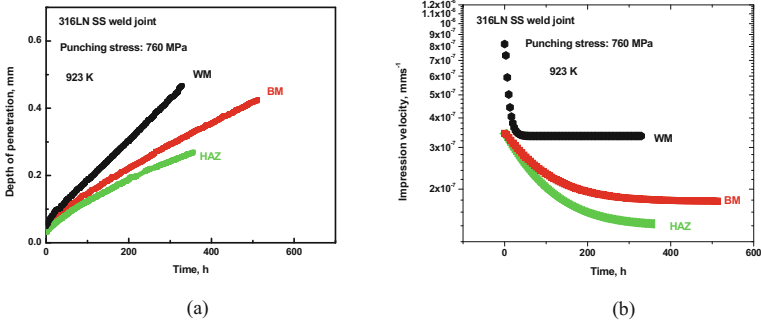
Fig. 3 a Typical IC curves for the weld metal, the base metal and the heat-affected zone of 316LN SS weld joint. **b** Impression velocity vs. time curves
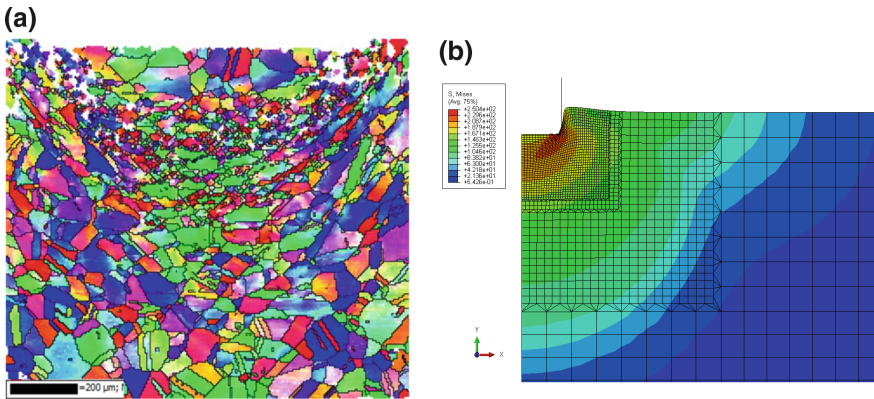
Fig. 4 a Electron back scatter diffraction image showing heterogenous deformation in 316LN SS under the punch after impression creep tests. **b** Von Mises stress distribution in the specimen showing maximum stress in the region associated with extensive shear deformation in 316LN SS

The heat-affected zones was found to have the lowest steady state impression velocity. These observations can be rationalized based on the differences in the microstructure and morphology of the three distinct regions in the weld joint.

Heterogeneity of Deformation in Impression Creep

The microstructural changes observed in the vicinity of the impression in 316LN stainless steel (SS) after the impression creep test is depicted in Fig. 4a which is an Electron Back Scatter Diffraction (EBSD) micrograph of the region under the indenter. Three distinct regions were observed. In the region immediately under the indenter, equiaxed grains with no significant change in grain shape were generally observed. This suggested that the stress acting in this region was hydrostatic in
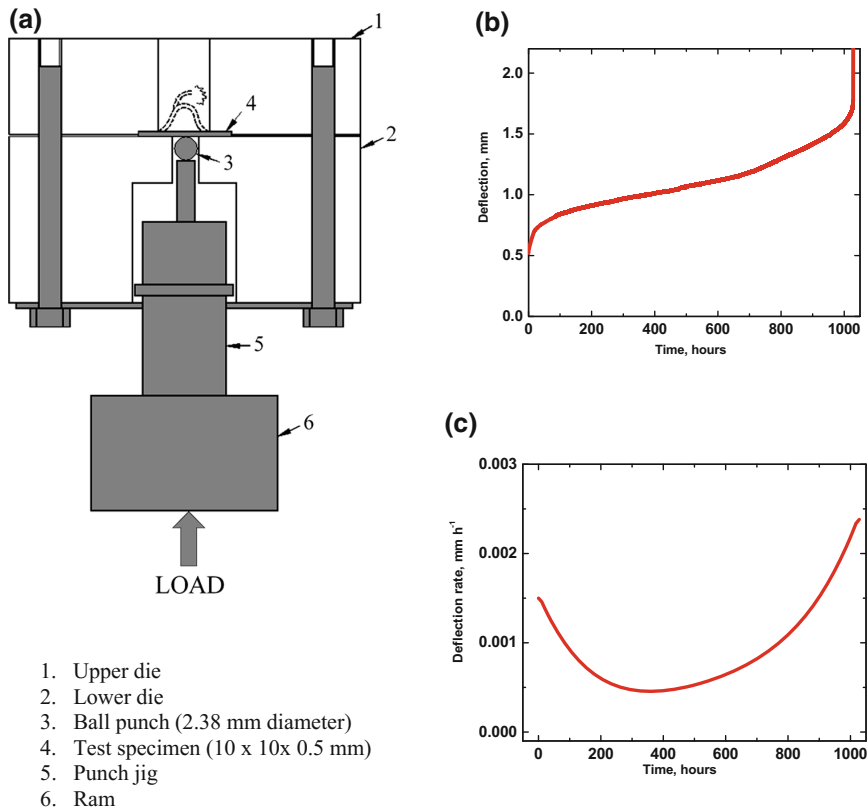
nature. The material in the region further below was found to have experienced extensive shear deformation. The region still further below which is far away from the indentation indicated equiaxed grains suggesting absence of plastic deformation in this region. This clearly demonstrates the localized nature of impression creep test. Finite element analysis of the region under the indenter showed that the Von Mises stress was maximum in the region which showed shear deformation as shown in Fig. 4b.

Small Punch Creep

Unlike Impression Creep, Small Punch Creep (SPC) test allows determination of creep fracture properties of materials also. Manahan and co-workers were the pioneers who developed the SPC test [11]. In SPC test, a small thin specimen of typical size $10 \times 10 \times 0.5$ mm is subjected to a constant load through a spherical ball indenter which is made of ceramic material and at high temperature. The deformation of the specimen is measured continuously as a function of time till the sample undergoes fracture. Under the action of the load, as the ball initially contacts the disc specimen, the specimen is subjected to elastic bending. Soon, plastic deformation occurs and the deformation front expands through the direction of the disc thickness and also radially outwards. This is followed by membrane stretching wherein the deformation front extends beyond the region of contact between the punch and the disc. The deformation continues at the constant load till the specimen develops a neck due to thinning and it finally leads to failure. Figure 5a shows schematically an SPC testing system.

The SPC curve is usually characterized by a loading strain and primary, secondary and tertiary creep stages. Figure 5b shows a typical SPC curve obtained on 316 LN SS at a load of 300 N at 923 K. A cross-plot of Fig. 5b in the form of variation of deflection rate with time is shown in Fig. 5c. The curve shows a minimum in the deflection versus rate curve. In SPC test, in the primary region, bending is the dominant mode of deformation whereas in the secondary and tertiary regions, membrane stretching is the dominant mode of deformation. The rapid increase in deflection rate in the tertiary region is on account of localization of deformation, and nucleation and growth of cracks. The variation of minimum deflection rate with load obeyed Norton power law just as in uniaxial creep. Rupture life increased linearly with decrease in load (on log-log scale). SPC rupture properties obeyed the Monkman-Grant relationship which relates the variation of minimum deflection rate as a function of rupture life just as in uniaxial creep.

Although the SPC parameters like minimum deflection rate and rupture life show the same kind of relationship with applied load as in the case of standard uniaxial creep tests using bulk specimens, it should be noted that SPC tests are carried out at constant load under bending conditions whereas standard uniaxial tests are carried out at constant nominal stress under axial loading. Further,

(a)

LOAD

1. Upper die
2. Lower die
3. Ball punch (2.38 mm diameter)
4. Test specimen (10 x 10x 0.5 mm)
5. Punch jig
6. Ram

Fig. 5 **a** Schematic of the Small Punch Creep experimental set-up. **b** SPC curve obtained on 316 LN SS at a load of 300 N at 923 K. **c** Variation of deflection rate with time derived from SPC curve obtained on 316 LN SS at a load of 300 N at 923 K

the stress state in SPC test is biaxial and is thus different from that in a uniaxial test. A valid relationship between data from SPC tests and standard uniaxial tests is therefore required. Figure 6a shows the variation of rupture life with SPC load. Superimposed in Fig. 6a are the data from conventional creep tests in the form of stress versus rupture life. Although a linear relationship is obeyed by both SPC and uniaxial data (on log-log scale), there is no correlation between SPC and uniaxial results. Several relationships have been proposed in the literature to correlate SPC rupture life with rupture life determined from uniaxial tests. Some of them are empirical in nature, while some are based on stretching membrane theory [13]. These correlation relationships contain several material and geometrical parameters. An empirical relationship which is obeyed by several engineering materials and which has been shown to have wide acceptance among the researchers, is given by $F/\sigma = K.R.t^2/h.D$ where F is the SPC load, σ represents the uniaxial stress, K is a constant, R is the radius of the punch diameter, t is the thickness of the specimen,
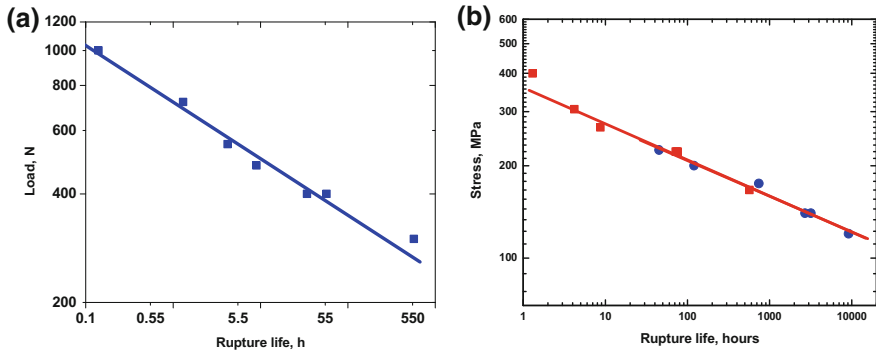
Fig. 6 a Variation of SPC rupture life with applied load for 316LN SS at 923 K. **b** Correlation of SPC rupture life with uniaxial rupture life [12]. *Red squares* represent SPC data and *blue circles* represent uniaxial creep data (Color figure online)

h is the radius of receiving hole and D is the ductility factor for the material in the test temperature and load range [14]. Taking into account the material and the geometrical parameters, the above equation can be simplified to the form $F/\sigma = \alpha$. Figure 6b shows the uniaxial and SPC rupture life data plotted in the same graph using the above relationship with a value of $\alpha = 1.8$. Since the values of D and K are not available, the value of α has been derived empirically by correlating SPC and uniaxial creep rupture life as recommended by CEN [15]. It shows an excellent correlation of the rupture life data from SPC and uniaxial creep tests and thus validates the SPC methodology to evaluate rupture life of materials. A value of $\alpha = 2.0$ has been reported for 316 SS [16] whereas a value of $\alpha = 1.4$ has been reported in the literature for grade 91 steel [17].

Alloy Development Studies Using SPC

SPC test technique was used for optimizing the amount of nitrogen in 316LN SS for superior creep properties [14]. SPC tests were carried out at 923 K on three heats of 316 LN SS containing 0.07, 0.11 and 0.14 wt% nitrogen. Figure 7a shows the variation of steady state deflection rate as a function of nitrogen content at various load levels. The minimum deflection rate decreased with increase in nitrogen content. Figure 7b shows the variation of rupture life with nitrogen content. Rupture life was found to increase with increase in nitrogen content. Both these results are consistent with the results obtained from separate uniaxial creep tests which showed a decrease in minimum creep rate and increase in rupture life with increase in nitrogen content [7]. These results clearly demonstrate that SPC test is an excellent and innovative technique to study creep properties of multiple heats with different compositions in relatively shorter test duration for the purpose of
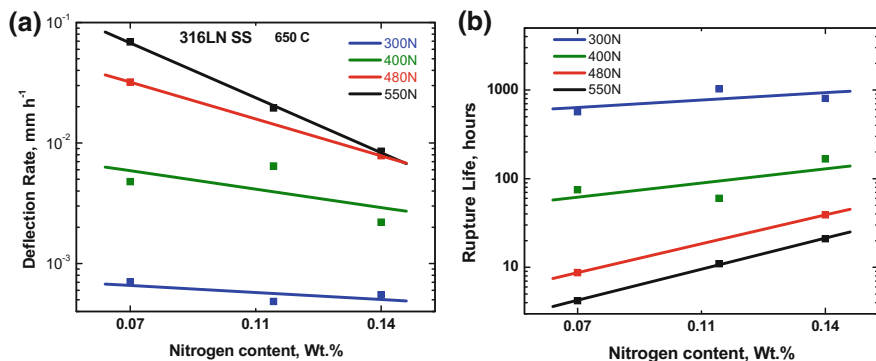
Fig. 7 **a** Influence of nitrogen content on steady state SPC deflection rate for 316LN SS at 923 K. **b** Influence of nitrogen content on SPC rupture life for 316LN SS at 923 K

optimizing chemical composition. In spite of the excellent correlations obtained between SPC and uniaxial data, it must be stated that there are several limitations to this technique. In SPC test, the type of loading is bending (SPC) unlike in conventional creep tests in which the loading is tensile. Further, the stress state is complex and multi-axial in SPC tests. The amount of material under the ball indenter which is undergoing elastic, plastic and creep deformation is not constant but is continuously varying. Nevertheless, the correlation with uniaxial data is good although it is still largely empirical.

Ball Indentation

Ball Indentation (BI) testing technique is an attractive small specimen testing method for estimating the hardness, tensile properties and fracture toughness of materials. It is based on strain-controlled multiple indentations at a single penetration location on a polished surface of a material (about $10 \times 10 \times 10$ mm size) using a small spherical indenter of diameter D (typically 1–2 mm). The applied indentation loads (P) and the associated penetration depths are measured continuously during the test, and the incremental stress-strain values are calculated by applying a combination of elasticity and plasticity theories, and semi-empirical relationships which govern material behavior under multiaxial indentation loading. The flow curve is analysed further and the yield strength, ultimate tensile strength, strength coefficient, strain hardening exponent and a fracture energy parameter called indentation energy to fracture are evaluated. The BI technique of loading followed by partial unloading during indentation enables a proper evaluation of indentation depth hp associated with plastic deformation of the material. The plastic diameter can then be determined from hp if the sinking-in and piling-up of the test material around the indentation are not pronounced [18]. In a standard tensile test,

Fig. 8 Typical load versus depth of penetration plot in a BI test. BI load increases approximately linearly with increase in penetration depth
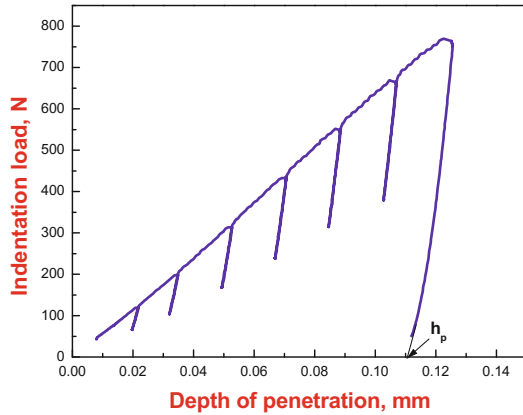

the uniaxial deformation is almost confined to the constant volume of the specimen's gauge section. Initially, the material is deformed elastically, following which plastic yielding and work-hardening commence, and these processes continue homogeneously till the onset of necking. In contrast, in a BI test, the elastic and plastic deformations are not distinctly separated; both elastic and plastic deformation take place simultaneously during the entire period of the test. With increasing indentation penetration depth, an increasing volume of test material is made to flow under multiaxial compressive stresses generated by the advancing indenter. BI load increases approximately linearly with penetration depth as shown in Fig. 8. The linear increase of load with depth of penetration is the consequence of two nonlinear but opposing processes occurring simultaneously; the nonlinear increase in the applied load with penetration depth because of the spherical geometry of the indenter, which is offset by the increase in load due to the work-hardening behavior of the material. For evaluating tensile properties of materials from BI tests, it is necessary to derive the true stress and true strain from BI data. The engineering parameters determined from tensile tests can be then evaluated. The theory of indentation and evaluation of true stress-true strain data as well as the tensile properties, from load-depth depth data, have been reported elsewhere [19]. Figure 9 shows an automated ball indentation system (schematic) used extensively by the author for carrying out extensive studies.

Indentation to Energy to Fracture

BI tests can also be used to estimate fracture energy of materials. The indentation does not induce any fracture in the material, since the stresses at the center of the contact surface of the test specimen under the indenter are compressive, whereas the stresses in front of a crack tip in a fracture specimen are tensile. However, elasticity theory and FE analyses have shown that the stress triaxilities present at a crack tip in a fracture toughness specimen and at the center of the contact surface under the

Fig. 9 Schematic of BI test set-up
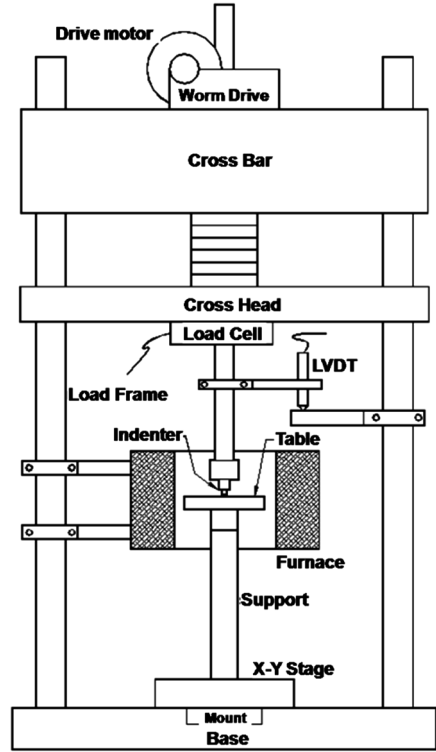
indenter are similar [20]. Therefore, the material at the center of the contact surface under the indenter experiences a degree of constraint similar to that experienced by the material at the crack tip. The deformation energy at the center of the impression is hence comparable to that at the front of a crack tip. Therefore, it has been proposed that the indentation energy per unit contact area up to a critical fracture stress is related to the fracture energy of a material in the transition region of an impact curve. This parameter is referred to as Indentation Energy to Fracture (IEF). The model assumes fracture conditions to occur if the stress produced by the ball indentation exceeds the material's critical cleavage fracture stress (σ_f). Hence if the value of stress at the point of contact is known as a function of indentation depth, the depth at which the stress exceeded σ_f could be predicted. If the energy deposited in the material by the indenter could be determined as a function of the depth, then the energy upto a depth equivalent to the assumed fracture stress could be estimated. This energy to fracture is termed the Indentation Energy to Fracture (IEF).

The expression for IEF is given as

$$IEF = \int_0^{h_f} \sigma_t(h)\,dh. \tag{5}$$

It represents the fracture energy as determined from ABI-measured load-depth curves up to either the critical fracture stress or strain, depending upon the controlling micromechanism causing fracture, which in turn depends on the test temperature. The concept of a critical fracture stress is applied to the transition region and the lower shelf region while the concept of a critical fracture strain is applied to the upper shelf region of a typical impact energy curve. From fracture mechanics models and generalized Griffith theory, it has been shown that the fracture toughness parameter K_{JC} can be related to the total indentation energy to fracture.

Ball Indentation Testing System

A typical BI system uses an electro-mechanically driven indenter, high resolution penetration transducer, load cell, a personal computer (PC), a 32-bit data acquisition/control unit, and a copyrighted ABI software. The test is fully automated with a PC and test controller used in innovative ways to control the test and analyze data including real-time graphics, digital display of load-depth test data, etc. Spherical indenters made of tungsten carbide are used with diameters varying from 0.254 to 1.575 mm, depending on the specimen thickness and width of the microstructural region to be tested. The indenter is driven at a constant speed into the material to be tested, and progressive multiple loadings/partial unloadings are performed at a single test location. Load and depth of penetration are monitored using on-line load cell and linear variable differential transducer respectively.

Ball Indentation Studies on Weld Joint

The unique advantage of using the BI technique lies in its ability to characterize narrow microstructural zones and gradients in mechanical properties of steel weld joints. Gradients in the strength of the base metal, weld metal and the different microstructural zones in the heat-affected zone were investigated on A533B pressure vessel steel weld joint prepared using submerged arc welding process [21]. Figure 10 depicts the variation of room temperature ultimate tensile strength with position from weld centre line, i.e., variation across weld metal, heat affected zone and base metal. The tensile properties were found to vary with changes in the microstructure in the weld metal, heat affected zone and base metal. The gradients in strength exhibited in the heat-affected zone could be correlated with the local microstructure as a function of the distance from the fusion line, such as coarse grain, fine grain and intercritical microstructural zones.
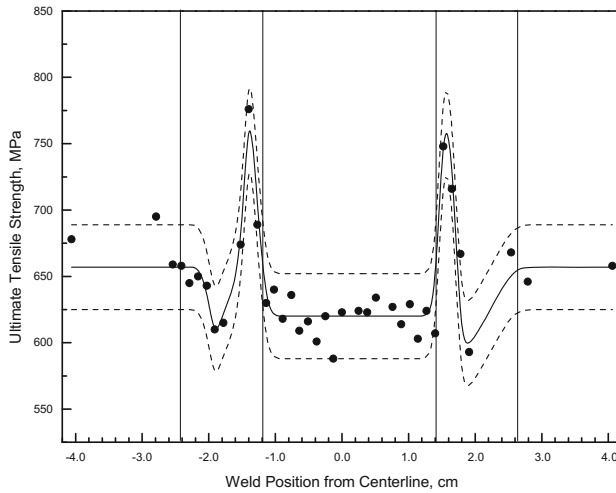
Fig. 10 Variation of room temperature ultimate tensile strength with position from weld centre line in A533 weld joint

Evaluation of Impact Energy and Fracture Toughness

Ball indentation technique can also be used to estimate fracture toughness of materials [22]. CF-8 is a cast austenitic stainless steel (SS) which is equivalent to wrought type 304 SS. Charpy tests were carried out on unaged, and 6 and 12 months aged materials using subsize specimens. Figure 11a shows the variation of Charpy impact energy C_V with test temperature for the unaged and aged materials. Twelve months aged material showed distinct lower-shelf and ductile to brittle transition regions. The upper shelf region was not well defined although tests were conducted up to 535 K. The unaged and 6 months aged materials showed only the transition regions over the range of test temperatures investigated. There was a significant drop in the impact energy following 6 months of aging. Indentation energy to fracture W_{IEF}, which is the fracture toughness parameter that is derived from ABI tests, was determined at each test temperature and in different material conditions. In determining the W_{IEF} values, a critical stress to fracture criterion was adopted and so the W_{IEF} values represent failure in the lower-shelf and transition regions of a typical impact energy versus temperature relationship. Figure 11b shows the variation of W_{IEF} with test temperature for unaged and aged materials using a value of 1200 MPa for σ_f. Regions of lower-shelf and ductile to brittle transition regions were observed for the unaged and all the aged conditions [23] Fig. 11c shows the correlation between C_V and WIEF. W_{IEF} increased linearly with C_V and so W_{IEF} values could be used to estimate C_V values.
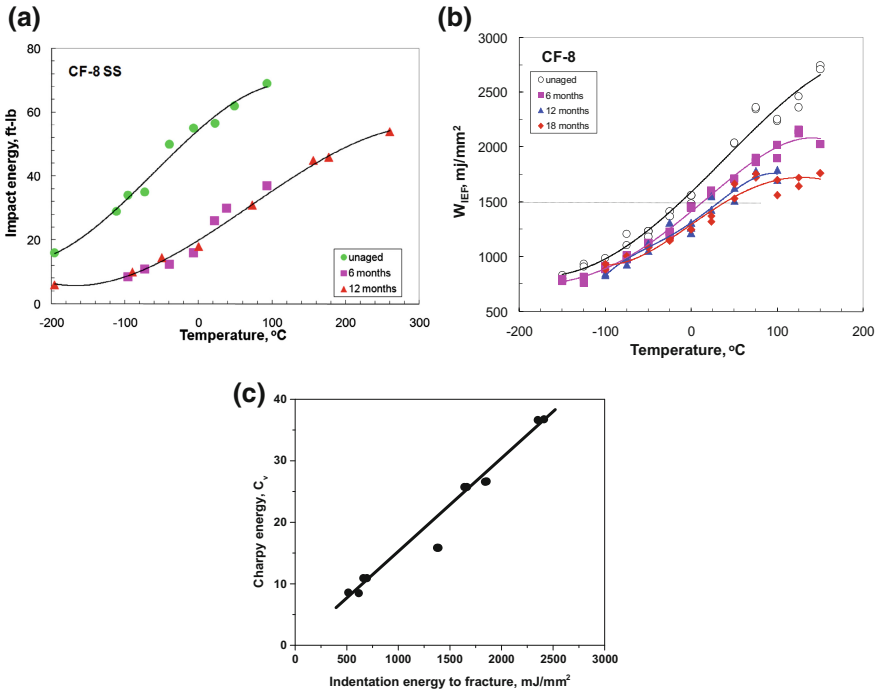
Fig. 11 a. Variation of Charpy impact energy C_V with test temperature for unaged and aged CF-8 SS. **b** Variation of indentation energy to fracture, W_{IEF} with test temperature for the unaged and aged CF-8 SS. **c** Correlation between Charpy impact energy C_V and indentation energy to fracture W_{IEF} for CF8 SS

Summary

Impression Creep, Small Punch Creep and Ball Indentation are innovative small specimen testing techniques that can be used to evaluate mechanical properties of materials with minimal amount of material. The results show good agreement with data from standard tests although certain amount of empiricism exists in the correlations. Through extensive finite element analysis, more meaningful correlations can be obtained. These techniques are very useful in assessing structural integrity of components, in alloy development and also to characterize the mechanical properties of narrow microstructural zones in weld joints. The steady state creep rates calculated from IC tests were found to be in good agreement with the steady state creep rates obtained using conventional uniaxial creep tests. Creep rupture life determined from SPC tests could be correlated with the rupture life determined from standard creep rupture tests. Tensile properties and fracture energy could be evaluated from BI tests.

References

1. J.C.M. Li, S.N.G. Chu, Scr. Mater. **13**, 1021 (1979)
2. F. Yang, J.C.M. Li, Mater. Sci. Eng. (R), **74**, 233 (2013)
3. J.C.M. Li, S.N. Chu, J. Mater. Sci. **12**, 2200 (1977)
4. Naveena, V.D. Vijayanand, V. Ganesan, K. Laha, and M.D. Mathew, Mater. Sci. Eng. A. **552,** 112 (2012)
5. D. Chiang, J.C.M. Li, J. Mater. Res. **9**, 903 (1994)
6. M.D. Mathew, Naveena and V.D. Vijayanand, J. Mater. Eng. Perform. **22** 492 (2013)
7. M.D. Mathew, K. Laha, V. Ganesan, Mater. Sci. Eng. A **535**, 76 (2012)
8. M.D. Mathew, V.S. Srinivasan, in *Mechanical Behavior of Nitrogen-bearing steels,* ed. by U. K Mudali, B. Raj. Monograph on High Nitrogen Steels and Stainless Steels (Narosa Publications, New Delhi, 2004), p. 182
9. W. Sun, T.H. Hyde, Creep analysis and failure prediction of welds. Acta. Metall. Sin. **12**, 68 (1999)
10. Naveena, V.D. Vijayanand, V. Ganesan, K. Laha, M.D. Mathew, Mater. Sci. Tech. (2014)
11. P. Manahan, A.S. Argon, O.K. Harling, J. Nucl. Mater. **103**, 1545 (1981)
12. M.D. Mathew, J. Ganesh Kumar, V. Ganesan, K. Laha, Small punch creep studies for optimisation of Nitrogen content in 316LN SS for enhanced creep resistance. Metall. Mater. Trans. A. **45**, 731–737 (2014)
13. S. Komazaki, T. Kato, Y. Kohno, H. Tanigawa, Mater. Sci. Eng. A. **511**, 229 (2009)
14. S. Komazaki, T. Hashida, T. Shoji, K. Suzuki, J. Test. Eval. **28**, 249 (2000)
15. Small Punch Test Method for Metallic Materials Part 1. *A Code of Practice for Small Punch Testing at Elevated Temperatures.* Report No. CEN/WS 21, (2005)
16. M.L. Saucedo-Munoz, S. Komazaki, T. Takahashi, T. Hashida, T. Shoji, J. Mater. Res. **17**, 1945 (2002)
17. D.T. Blagoeva, R.C. Hurst, Mater. Sci. Eng. A. **511**, 219 (2009)
18. C.H. Mok, Exp. Mech. **6**, 87 (1966)
19. M.D. Mathew, Naveena, J. Ganesh Kumar, Trans. Indian Inst. Met. (2016). doi:10.1007/s12666-016-0847-2
20. F. Haggag, T.-S. Byun, J. Hong, P. Miraglia, K.L. Murty, Scripta Mater. **38**, 645 (1998)
21. K.L. Murty, P.Q. Miraglia, M.D. Mathew, V.N. Shah, F.M. Haggag, Int. J. Press. Vess. Pip. **76**, 361 (1999)
22. M.D. Mathew, K.L. Murty, J. Mater. Sci. **34**, 1497 (1999)
23. M.D. Mathew, L.M. Lietzan, K.L. Murty, V.N. Shah, Low temperature aging embrittlement of CF-8 stainless steel. Mater. Sci. Eng. **269**, 186–196 (1999)